U Karst
Volume 09 Number 01 Year 2025

ISSN (*Online*) 2581-0855
ISSN (*Print*) 2579-4620

Available Online at
https://ojs.unik-kediri.ac.id/index.php/ukarst/index

https://dx.doi.org/10.30737/ukarst.v9i1.6587

Landslide Mechanisms in the Cisumdawu Toll Road through a Geoforensics Approach to Increase Slope Stability

A. Mardjuni[1*], P. P. Rahardjo[2], F. Aldiamar[3]

[1*,2]*Civil Engineering Department, Faculty of Engineering, Parahyangan Catholic University, Bandung, Indonesia*

[1*]*National Road Implementation Agency for DKI Jakarta - West Java Region, Directorate General of Highways, Ministry of Public Works, Indonesia*

[3]*Directorate of Freeways, Directorate General of Highways, Ministry of Public Works, Indonesia*

Email: [1*]adhystira@pu.go.id, [2] paulus.rahardjo@unpar.ac.id, [3]fahmi.aldiamar@pu.go.id

ARTICLE INFO

Article History :
Article entry : 14 – 02 – 2025
Article revised : 07 – 04 – 2025
Article received : 24 – 04 – 2025

Keywords :
Geoforensics, Groundwater Level, Landslide, Lateral Presure Coefficient (K0).

IEEE Style in citing this article :
A. Mardjuni, P. P. Rahardjo, and F. Aldiamar, "Landslide Mechanisms in the Cisundawu Toll Road through a Geoforensics Approach to Increase Slope Stability," U Karst, vol 9, no. 1, pp 46 – 61, 2025, doi: 10.30737/ukarst.v9i1.6587

ABSTRACT

Landslides are a significant threat to infrastructure in tropical regions like Indonesia, especially in projects that cross volcanic slopes. A significant case occurred on the Cisumdawu Toll Road Section 2, triggered by high rainfall and water-saturated young volcanic soil. Given the complexity of such failures, comprehensive investigations are crucial. This study aims to analyze the causes and mechanisms of landslides in the Ciherang Village, specifically at STA 19 KM 65 using a geoforensics approach. This approach involves field investigations to collect geotechnical and geophysical data such as boring logs, SPT, pressure meters, inclinometers, and geoelectric resistivity testing. These were used to reconstruct subsurface conditions before failure. Numerical modeling was then performed with variations in groundwater level (GWL) and K_0 to simulate slope stability and identify failure triggers. The results show that landslides was translational, occurring in the transition zone between sandy silt (tuff) and weathered tuff breccia layers at depths of 30–35 meters, where differences in permeability made the zone vulnerable. The decrease in GWL significantly improved slope stability, increasing the safety factor to 1.435, while K_0 variation had a lesser impact. A combination of bored piles, ground anchors, soil nailing, and slope regrading effectively stabilized the slopes. These findings contribute to a better understanding of the mechanisms and causes of landslides so that mitigation strategies can be more targeted to increase slope stability.

U Karst
Volume 09 Number 01 Year 2025
ISSN (*Online*) 2581-0855
ISSN (*Print*) 2579-4620

1. Introduction

Landslide disaster is one of the geotechnical phenomena that often occurs globally. In 2022, it was recorded that there were approximately 100 landslides in West Java. In tropical countries such as Indonesia, landslides have become a critical issue affecting civil infrastructure, especially highway, railway, and dam construction projects that cross hills or mountains [1]. Slope failures in such infrastructure cause structural damage, disrupt regional connectivity, and potentially cause large-scale economic losses and safety risks for the community [2]–[4]. One of the significant cases of slope failure occurred in the Cisumdawu Toll Road Section 2 construction project, precisely at STA 19 (KM 175), which is located in the Ciherang Village area, South Sumedang District, Sumedang Regency [5]. In February 2022, when the rainfall intensity was high, a large landslide occurred in the excavation area with a depth of ± 60 meters with a distribution length of ± 150 meters. The landslide crown originated from the 9th slope with a height of about 54 meters from the road elevation. In addition to the main landslide, the phenomenon of uplift of the road body as high as 19 cm was also recorded in the period from March to May 2022. This location is in an area with young volcanic soil lithology, which naturally has weak cementation and is very sensitive to water, so it is easily weathered and decreases in shear strength when saturated. The combination of geological, hydrological conditions, and large-scale excavation activities makes this zone highly susceptible to landslides.

Various approaches have been developed to address landslides, such as empirical methods, conventional stability analysis, and numerical modeling. These approaches are often unable to explain complex failure mechanisms, especially in tropical volcanic soils. The geoforensics engineering approach is a more comprehensive method integrating geotechnical, geophysical, and numerical analysis data to understand the causes and mechanisms of landslides in more depth. Geoforensics combines geotechnical engineering analysis with a retrospective investigative approach to accurately reconstruct and understand the causes of failure. This approach identifies interactions between geotechnical parameters such as groundwater table changes, construction loads, and weathered or naturally disturbed soil conditions. By compiling technical evidence from multiple field data sources and linking it to the actual behavior of slopes during landslides, geoforensics can provide a deeper understanding of failure mechanisms and provide a strong technical basis for more targeted mitigation and re-planning recommendations.

Several previous studies have applied this approach with significant results in understanding the behavior of unstable slopes. Integrating geotechnical data, stratigraphic

https://dx.doi.org/10.30737/ukarst.v9i1.6587

U Karst
Volume 09 Number 01 Year 2025
ISSN (*Online*) 2581-0855
ISSN (*Print*) 2579-4620

interpretation, and numerical modeling successfully revealed the role of weathered rock zones and slope configuration on landslides on the Mediterranean Ring Road in Morocco [6]. Studies in the Himalayan region highlight the importance of combining geotechnical and geophysical investigations to analyze land subsidence due to heterogeneous soil structures and deep weathering [7]. In addition, machine learning can be used to map landslide vulnerability with high accuracy in mountainous areas [8]. This mapping provides spatial information about potential risks and helps in evidence-based mitigation decision-making [9]. In addition, the geological approach also provides important insights into understanding landslide mechanisms. Rock weathering and fracture systems forming weak zones that accelerate water infiltration can trigger landslides [10]. Geological structure, slope morphology, and subsurface conditions are very important to consider in landslide mechanisms [11].

Although the geoforensics approach has shown effectiveness in understanding landslide events in various regions, its application to tropical volcanic soils is still very limited. This study aims to analyze the causes and mechanisms of landslides in the Ciherang Village, specifically at STA 19 KM 65, using a geoforensics approach. This study will focus on volcanic soils by considering the influence of the K_0 value. This study is expected to provide a strong basis for understanding the mechanisms and causes of landslides, so that the designed mitigation strategies are more targeted in increasing slope stability, reducing the risk of infrastructure damage, and protecting public safety.

2. Research Method

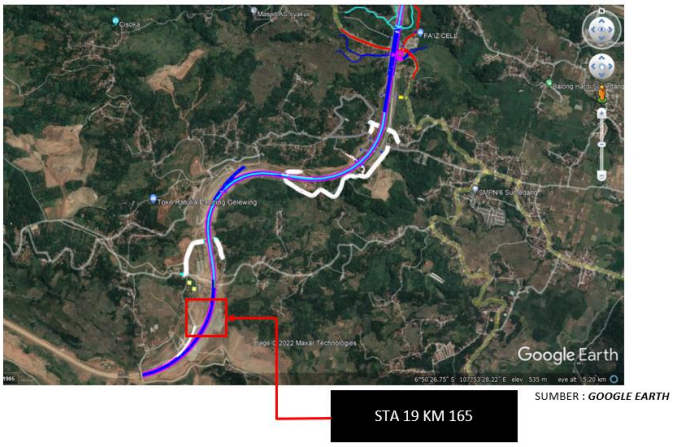

Source: Google Earth (2024).

Figure 1. Location Map

This research was conducted at the Cisumdawu Toll Road Section 2 landslide site in Ciherang Village, South Sumedang District, Sumedang Regency. The research began with

https://dx.doi.org/10.30737/ukarst.v9i1.6587

ISSN (*Online*) 2581-0855
ISSN (*Print*) 2579-4620

collecting field data from log drilling, soil laboratory tests, geoelectric resistivity measurements, and deformation monitoring using an inclinometer. In addition, numerical modeling was carried out to analyze slope stability with and without reinforcement, and to evaluate slope sensitivity to changes in groundwater levels and K_0 values. Furthermore, the modeling results were examined thoroughly to identify slip planes and assess the effectiveness of the reinforcement system.

2.1 Data Collection

Data obtained from the results of field investigations conducted by the Service Provider for the Cisumdawu Toll Road Construction Project Section 2 Phase II. The data obtained includes drill log data, SPT (Standard Penetration Test), geoelectric data, Pressure meter Test data, and inclinometer monitoring data that records deformation/movement. The data will be used in data analysis. Drilling was carried out at 8 (eight) points at the work location.

Table 1. Drill Point Location

No	Drill Location	Depth
1	STA 19+725 BH 01 A	15 m
2	STA 19+775 BH 01 B	20 m
3	STA 19+810 BH 02	20 m
4	STA 19+825 BH 03 A	30 m
5	STA 19+850 BH 03 B	30 m
6	STA 19+810 BH 06	20 m
7	STA 19+825 BH 07	30 m
8	STA 19+800 BH 5	40 m

Source: Author Research Data (2025).

2.2 Modelling

Numerical modeling was performed to evaluate the slope stability before and after treatment. Modeling was carried out using Plaxis 2D 2023 software, with Finite Element Method analysis to model the geometric conditions of the slope, soil properties based on test data, and actual hydrological conditions [12]. The stability criteria used are SF ≥ 1.25 according to SNI 8460-2017. The simulation scenario is carried out by considering variations in groundwater level (GWL) conditions such as existing GWL, GWL -2m, GWL -4m, and GWL -6m. In addition, the K_0 scenario includes K_0 -0.3, K_0 -0.2, K_0 -0.1, existing K_0, K_0 +0.1, K_0 +0.2, and K_0 +0.3. These variations are used to understand the interaction of changes in GWL and K_0 on the safety factor (SF). This modeling will also use a reinforcement system in stages such as bored piles, regrading, ground anchors, and soil nailing. This modeling is also used to visualize the distribution of deformation, stress, and the position of the critical slip plane.

https://dx.doi.org/10.30737/ukarst.v9i1.6587

U Karst
Volume 09 Number 01 Year 2025
ISSN (*Online*) 2581-0855
ISSN (*Print*) 2579-4620

2.3 Data Analysis

Based on the data that has been collected, the soil stratigraphy, groundwater level, and K_0 parameters will be obtained. Data from monitoring, soil testing, and modeling are analyzed in an integrated manner to reconstruct the slope failure mechanism. Stratigraphic interpretation is used to identify potential weak zones. From back analysis, it was found that some of the soil parameters before soil failure occurred (c and ϕ) when SF approached the value of 1 with the slip plane at the same location as the inclinometer. Inclinometer results are analyzed to determine the depth and value of the most significant movement. The safety factor (SF) values from modeling are compared in each scenario to assess the effectiveness of the handling [13]. Then after obtaining the stability analysis when the landslide occurred, re-modeling was carried out to get a simulation of the stability of the reinforced soil, in addition to the K0 sensitivity analysis. Sensitivity analysis on GWL and K_0 was conducted to evaluate the effect of changes in soil conditions on slope stability. The results were analyzed to provide technical justification for the landslide mechanism that occurred and recommendations for handling.

3. Results and Discussions

3.1 Geoelectric and Hydrogeological Characteristics

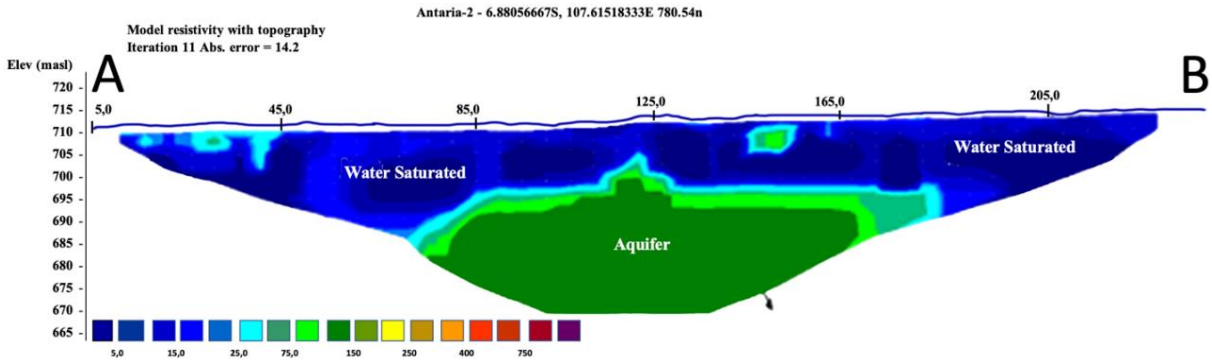

Source: Author Research Results (2025).

Figure 2. Subsurface Cross

Using the geoelectric resistivity method, the results of geophysical testing on the A–B line indicate that most subsurface layers are classified as water-saturated layers and shallow aquifers. This finding aligns with the local geomorphological conditions, which are volcanic areas with high rainfall and large infiltration capacity. The resistivity value indicates that most soil layers have low resistivity values, which strengthens the suspicion of high pore water content (**Figure 2**).

This saturation condition is crucial in the context of slope stability. Previous studies have shown that high groundwater levels can reduce the effective stress in the soil mass, thereby

https://dx.doi.org/10.30737/ukarst.v9i1.6587

ISSN (*Online*) 2581-0855
ISSN (*Print*) 2579-4620

reducing the shear strength and triggering failure on the potential slip plane [14]–[16]. In volcanic soils, especially those formed in humid tropical climates, this effect is even more pronounced due to their high porosity and sensitivity to water. Continuous groundwater flow also contributes to high pore pressure. This phenomenon is confirmed by field observations showing the emergence of springs and active seepage on the slope surface.

3.2 Subsurface Stratigraphy and Soil Classification

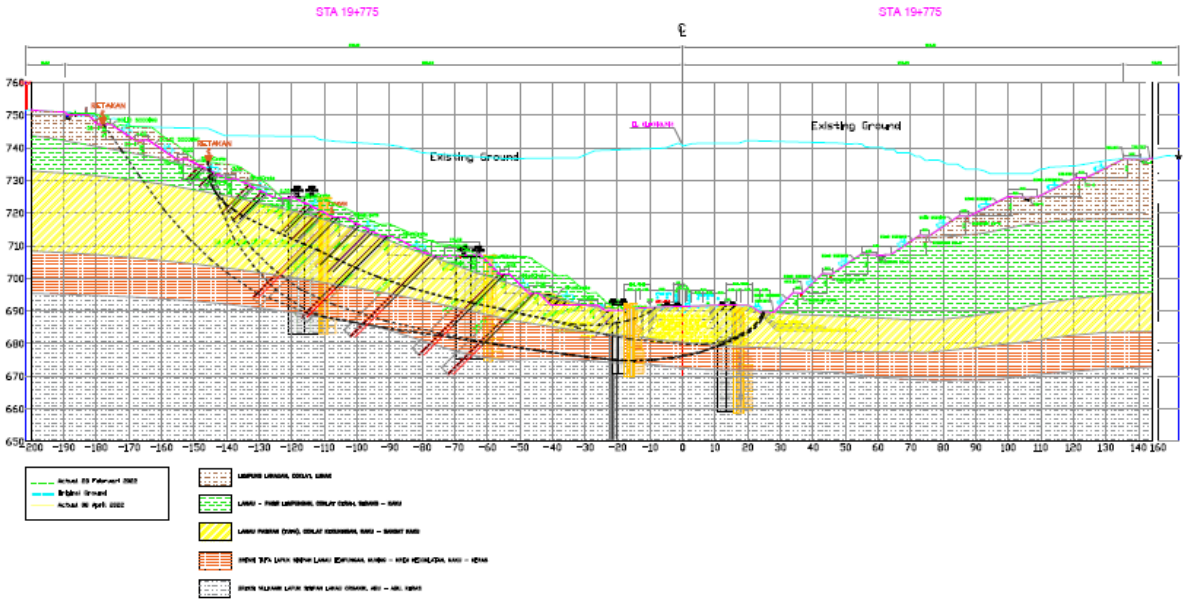

Source: Author Research Results (2025).

Figure 3. Cross Section

Table 2. Soil Classification Based on Stratigraphy STA 19+775 (1)

Elevation	Soil Type	Color	Consistency
750 – 744	Silty Clay	Chocolate	Soft
744 – 732	Silt – Clay Sand	Red Chocolate	Medium – Stiff
732 – 708	Sandy Silt (Tuff)	Fawn	Stiff – Very Stiff
708 – 695	Intercalated Wathered Tuff Breccia Silt Clay	Yellow – Brownish Cream	Stiff - Hard

Source: Author Research Results (2025).

Stratigraphic information was obtained from cross-sections from a combination of drill logs, geoelectric data, and inclinometers at STA 19+775 (**Figure 3** and **Table 2**). The vertical distribution of the material shows a gradual transition from soft to hard layers at a depth of about 30 meters, indicating a potential zone of weakness at a depth of between 20 and 30 meters, especially at the interface between sandy silt and weathered tuff breccia.

Table 3. Soil Classification Based on Stratigraphy STA 19+775 (2)

Soil Type	Specific Gravity (kN/m^2)	c'(kN/m^2)	ø' (')	E'50 (kN/m^2)	Eur (kN/m^2)
Silty Clay	18	20	20	18 x 10^3	36 x 10^3

https://dx.doi.org/10.30737/ukarst.v9i1.6587

U Karst
ISSN (*Online*) 2581-0855
Volume 09 Number 01 Year 2025
ISSN (*Print*) 2579-4620

Silt – Clay Sand	18	26	26	50×10^3	100×10^3
Sandy Silt (Tuff)	18	45	30	100×10^3	200×10^3
Intercalated Wathered Tuff Breccia Silt Clay	17	15	15	18×10^3	36×10^3

Source: Author Research Results (2025).

This classification shows that each layer has different shear strength and elastic modulus parameters, which will affect the overall slope deformation behavior (**Table 3)**. In addition, the characteristics of volcanic soil at the study site, especially in the tuff layer, tend to weaken drastically due to water saturation [17], [18].

3.3 Deformation Analysis Based on Inclinometer

The monitoring results show a significant pattern of ground movement with varying depths and magnitudes of deformation between locations (**Table 4**).

Table 4. Inclinometer Monitoring Results

STA	No INC	Number of Readings	Largest Land Movement (m)	mm
19+810	01	9 times	35 – 40	20,14
19+800	04	8 times	30 – 35	47,08
19+775	05	11 times	30 – 35	52,96
19+810CL	06	11 times	45 – 50	46,80
19+825	07	8 times	35 - 40	34,54

Source: Author Research Results (2025).

The INC 05 inclinometer recorded a maximum movement of 52.96 mm at a depth of 30–35 meters, the most significant deformation of all observation points. This indicates that in this zone there is an active slip plane that has the potential to become a landslide initiation area. In general, most deformations were detected at depths between 30–50 meters, with the direction of movement parallel to the slope gradient. These data indicate that the main slip plane is in the transition zone between the sandy silt layer (tuff) and the weathered tuff breccia, which geotechnically is a low-strength boundary due to differences in physical and mechanical characteristics between layers.

3.4 K0 Value Based on Pressuremeter Test

The K_o values obtained sequentially are 0.83 for the first layer (silty clay), 1.00 for the second layer (silty-sand clay), and 1.12 for the third layer (sandy silt/tuff). The high K_o values in these layers indicate the characteristics of overconsolidated volcanic soil with a high overconsolidation ratio (OCR) due to the influence of geological stress and old weathering processes. Volcanic soil is known to have a dense internal structure and experiences preloading from historical pressure, resulting in a higher lateral stress value compared to normal consolidated clay soil [19], [20].

3.5 Numerical Modeling and Evaluation of Slope Handling Effectiveness

https://dx.doi.org/10.30737/ukarst.v9i1.6587

ISSN (*Online*) 2581-0855
ISSN (*Print*) 2579-4620

The analysis results show that the initial condition of the slope before reinforcement had a safety factor (SF) value of 1.063 (**Figure 4**), indicating the stability limit condition and high vulnerability to slope failure. The gradual application of the reinforcement system resulted in a significant increase in the SF value. The installation of bored piles resulted in an increase in the SF to 1.106. The SF value increased again to 1.227 after regrading. After implementing the final reinforcement system in the form of ground anchors and soil nailing, the SF reached a value of 1.288, which met the required planning criteria.

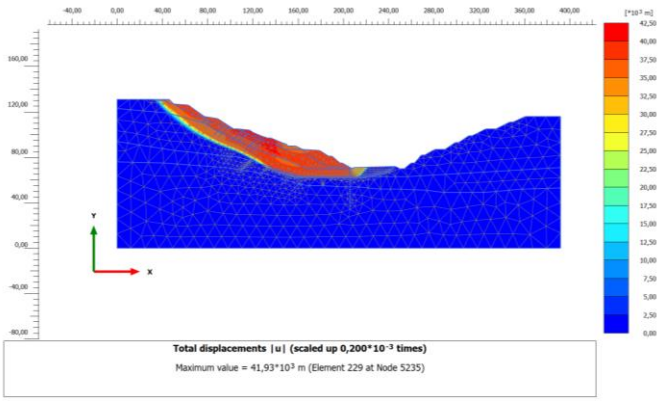

Source: Author Research Results (2025).

Figure 4. Main Modeling (SF Initial 1,063)

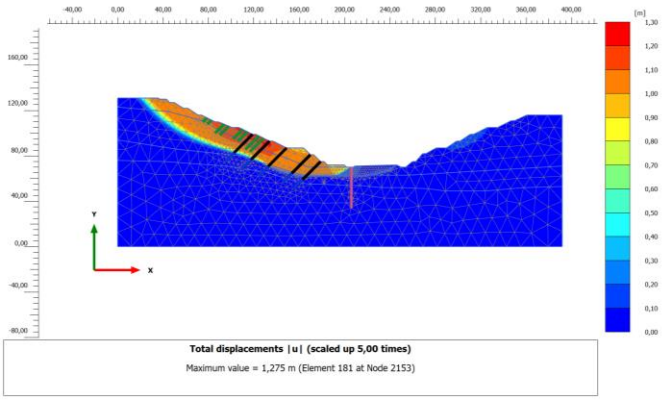

Source: Author Research Results (2025).

Figure 5. Primary Modeling (SF 1.288)

The initial condition of the slope shows that the maximum deformation zone is located at a depth of about 30 meters from the surface, indicating a potential for dominant failure in the transition zone between weak soil layers. The pattern of soil movement is lateral and concentrated on the slip plane. After the implementation of the reinforcement system in stages, including the installation of bored piles, regrading, and the application of ground anchors, the SF value increased to 1.288, as shown in Figure 4. The deformation distribution became more limited and concentrated in deeper areas, indicating the success of the intervention in cutting the landslide path and improving the slope structure. The increase in the SF value indicates the

https://dx.doi.org/10.30737/ukarst.v9i1.6587

U Karst
Volume 09 Number 01 Year 2025
ISSN (*Online*) 2581-0855
ISSN (*Print*) 2579-4620

success of soil reinforcement and can stabilize the critical slip plane trajectory [21], [22]. The modeling results show that the reinforcement elements effectively cut the landslide propagation path, reduce stress concentration, and increase the slope bearing capacity. This is supported by the results of the stress ratio distribution. In the initial condition (**Figure 5**), large areas with stress ratio values close to 1 (marked in red and orange) indicate zones where the shear stress almost exceeds the shear strength of the soil. After treatment (**Figure 6**), the critical zone experienced a drastic shrinkage, with a lower and more widespread stress ratio distribution, indicating a stress redistribution towards a more stable condition.

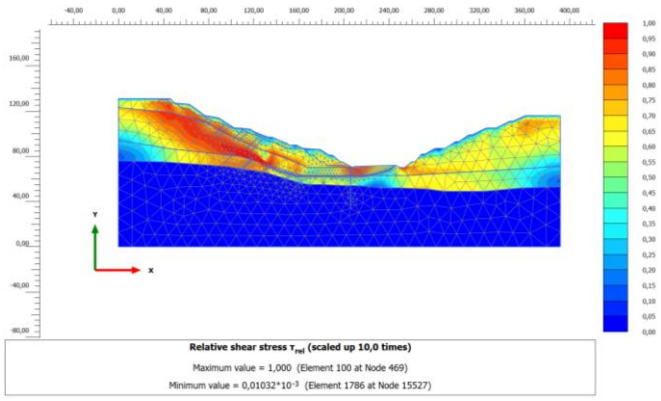

Source: Author Research Results (2025).

Figure 6. Stress Ratio Before Handling

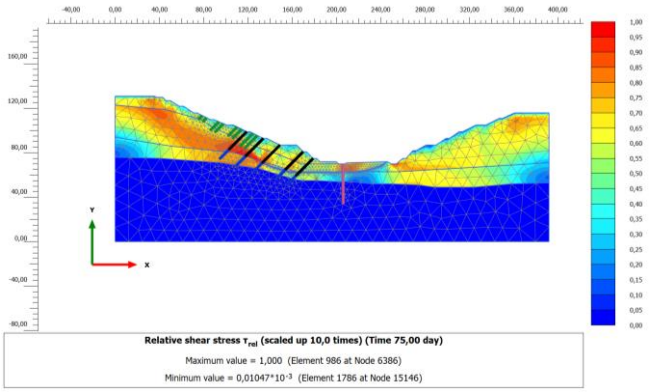

Source: Author Research Results (2025).

Figure 7. Stress Ratio After Handling

The modeling results show that the ground motion is concentrated in certain weak zones, forming a slip plane with an incomplete trajectory. This phenomenon indicates that the failure mechanism tends to be local and limited, rather than a general mass movement as assumed in conventional empirical approaches. This is consistent with the ground motion pattern recorded by the inclinometer and the interpretation of subsurface stratigraphy. The numerical modeling results confirm the effectiveness of the applied reinforcement system and show the deformation behavior and stress distribution in the slope. The modeling results show

https://dx.doi.org/10.30737/ukarst.v9i1.6587

ISSN (*Online*) 2581-0855
ISSN (*Print*) 2579-4620

that the ground movement is concentrated in certain weak zones, forming a slip plane with an incomplete trajectory. This phenomenon indicates that the failure mechanism tends to be local and limited, not a general mass movement as assumed in the conventional empirical approach [23], [24].

3.6 Sensitivity Analysis of Groundwater Level (GWL)

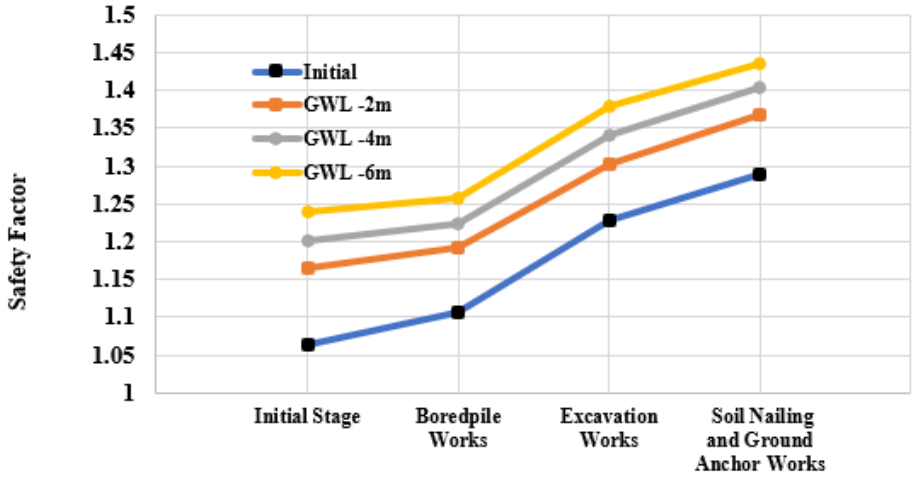

Source: Author Research Results (2025).

Figure 8. Comparison Chart of SF Values by Work Type

Figure 8 shows a consistent increasing trend of SF along with the decrease in groundwater level at all stages, starting from the initial condition to after the application of the final reinforcement system. At the initial condition, the SF value ranges from 1.063. When the GWL is lowered by 2 meters, the SF value increases to 1.165, and continues to increase to 1.239 when the GWL is lowered to 6 meters. A similar trend is also observed at the stages of bored pile work, excavation, and installation of soil nailing and ground anchors. At the final stage, the highest SF value reaches 1.435 at the lowest GWL condition (6 m), compared to 1.288 at the existing groundwater level condition.

The curve pattern on the graph shows that each decrease in the groundwater level positively contributes to increasing stability, with the highest increase occurring at the excavation stage and after final reinforcement. The decrease in GWL contributes to increasing the effective stress (σ′), thereby increasing the shear capacity of the soil [25]–[27]. In volcanic soils with high sensitivity to saturation, pore water's influence is dominant in reducing soil strength. Therefore, the GWL reduction strategy has proven effective as a mitigative approach that not only strengthens slope stability but also increases the efficiency of the applied reinforcement system. Planning a drainage system that can maintain groundwater levels at a safe depth can be used as a slope management strategy, especially in areas with volcanic soil and high rainfall. Reducing GWL is carried out by arranging drainage and drilling wells.

https://dx.doi.org/10.30737/ukarst.v9i1.6587

U Karst
Volume 09 Number 01 Year 2025
ISSN (*Online*) 2581-0855
ISSN (*Print*) 2579-4620

3.7 Sensitivity Analysis of K_0 Value

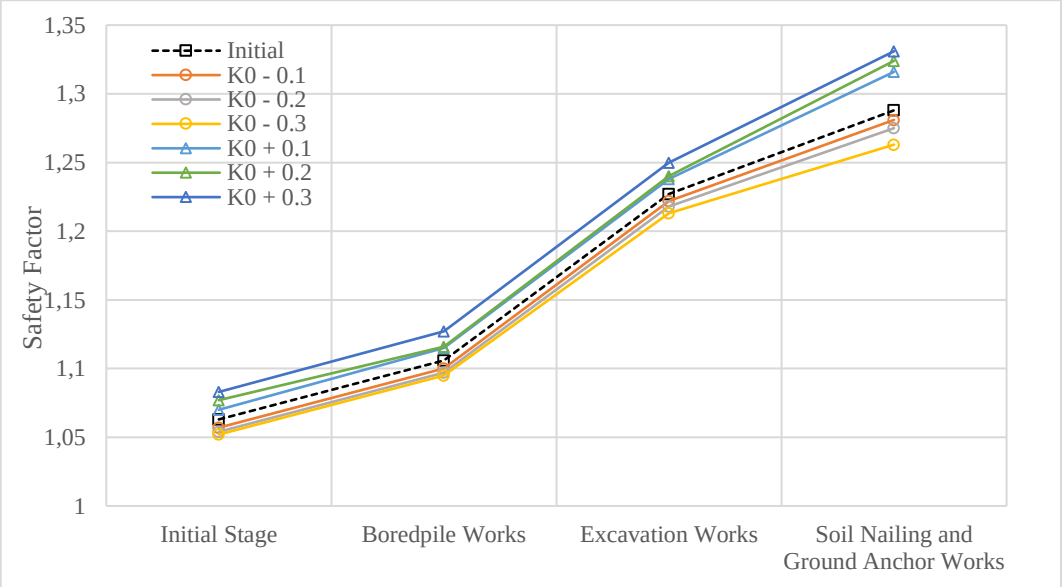

Source: Author Research Results (2025).

Figure 9. SF Value Graph for Each Type of Job

The simulation results show that variations in the K_0 value impact the safety factor (SF) value, although the sensitivity level is relatively lower compared to the influence of groundwater level (GWL). The modeling results show that an increase generally follows an increase in the K_0 value in the SF value. Conversely, a decrease in the K_0 value causes a decrease in SF at all stages of work. In the final stage after reinforcement (soil nailing and ground anchor), the SF value increases from 1.288 (existing K_0) to 1.331 when K_0 is increased by 0.3. Conversely, when K_0 is decreased by 0.3, the SF value decreases to 1.263. Increasing K_0 causes an increase in effective lateral stress (σ'_h), which increases effective average pressure (p').

3.8 Failure Mechanisms and Engineering Implications

The landslide mechanism at the study site results from a complex interaction between the geotechnical conditions of volcanic soil, groundwater table dynamics, and changes in the geometric configuration of the slope due to excavation activities. The slope failure was not comprehensive, but was limited to the transition zone between layers, which was characterized by significant differences in mechanical characteristics, especially between the sandy silt (tuff) layer and the weathered tuff breccia. Inclinometer data showed that the active slip plane was concentrated at a depth of 30–35 meters, which corresponds to the position of the weathered material transition zone. The recorded ground motion was horizontal and localized, supporting the interpretation that the landslide occurred through a translational mechanism on the slip plane. This was confirmed by the results of numerical modeling, which showed the area's dominant deformation distribution and stress ratio. This study strengthens previous studies by

https://dx.doi.org/10.30737/ukarst.v9i1.6587

ISSN (*Online*) 2581-0855
ISSN (*Print*) 2579-4620

proving that slope failure is triggered by failure in the transition zone with a difference in permeability. So it can be said that landslides do not always occur throughout the land, but only in some locations, such as slip planes. Slope stability is also influenced by the K_0 parameter.

The increase in the safety factor (SF) from 1.063 to 1.288 after reinforcement, as well as the decrease in the maximum deformation value from 41.97 cm to 12.75 cm, proves the effectiveness of the gradual stabilization system applied. The distribution of stress ratios that show a decrease in the critical zone after treatment emphasizes the success of the intervention in reducing stress concentrations that have the potential to trigger failure. In addition, the sensitivity analysis results on the groundwater level (GWL) show that the gradual decrease in GWL contributes significantly to the increase in SF to reach 1.435. This indicates that soil saturation is a dominant factor in reducing the shear strength of volcanic soils, and control of the groundwater level should be a priority in the design of slope stabilization in similar areas. Meanwhile, variations in the K_0 value also show an effect on stability, although with a lower level of sensitivity than GWL.

The overall analysis found that the failure mechanism was multi-factorial, dominated by hydrogeological conditions and volcanic soil characteristics that are very sensitive to saturation. Changes in slope configuration due to excavation accelerated the soil mobilization process in weak zones undergoing advanced weathering. In other words, landslides were triggered by the accumulation of pore water pressure in unbalanced geometric conditions, in soil media with fragile structures due to geological processes. The engineering implications of these findings emphasize the importance of implementing an adaptive drainage system to maintain groundwater level stability, in situ validation of soil stress parameters (such as K_0), and using a geoforensics approach to analyze failures and develop evidence-based mitigation strategies. This approach has proven to provide a comprehensive understanding of the causes of landslides and produce more contextual and effective technical recommendations in tropical volcanic soil conditions.

4. Conclusion

Based on the results of geoforensics investigations on landslides on the Cisumdawu Toll Road, it was found that slope failure was triggered by a complex interaction between tropical volcanic soil saturation and water springs, excavation geometry configuration, and differences in mechanical characteristics between subsurface layers. The identified landslide mechanism is translational in the transition zone between sandy silt (tuff) and weathered tuff breccia at a depth of 30–35 meters, reinforced by evidence of lateral deformation from

https://dx.doi.org/10.30737/ukarst.v9i1.6587

ISSN (*Online*) 2581-0855
ISSN (*Print*) 2579-4620

inclinometers and numerical modeling. The decrease in groundwater level was proven to be significant in increasing slope stability, as indicated by an increase in the safety factor of up to 1.435, while variations in the K_o value also affected stability, although with lower sensitivity. Implementing a gradual reinforcement system through bored piles, regrading, ground anchors, and soil nailing successfully inhibited deformation propagation and improved stress distribution in the soil mass. These findings provide a strong basis for understanding the mechanisms and causes of landslides, so that the mitigation strategies developed are more targeted to increase slope stability.

5. Acknowledgement

The author would like to thank Satuan Kerja Pelaksanaan Jalan Bebas Hambatan Provinsi Jawa Barat, National Road Implementation Agency for DKI Jakarta—West Java Region, Directorate of Freeways, Directorat General of Highways, and Parahyangan Catholic University for providing and supporting the author during the writing process.

References

[1] S. L. Gariano and F. Guzzetti, "Landslides in a changing climate," *Earth-Science Rev.*, vol. 162, pp. 227–252, 2016, doi: 10.1016/j.earscirev.2016.08.011.

[2] R. Pratama, "Kondisi Tanah Gembur Jadi Kendala Evakuasi Korban Longsor di Cangar-Pacet Mojokerto," 2025. https://www.suarasurabaya.net/kelanakota/2025/kondisi-tanah-gembur-jadi-kendala-evakuasi-korban-longsor-di-cangar-pacet-mojokerto/

[3] Tempo.com, "5 Bencana Longsor di Berbagai Daerah di Indonesia pada Januari 2025," 2025. https://www.tempo.co/politik/5-bencana-longsor-di-berbagai-daerah-di-indonesia-pada-januari-2025-1197448

[4] detik.com, "Detik-detik Kaki Korban Ditemukan Tertimbun Longsor Jalur Pacet-Cangar," 2025. https://www.detik.com/jatim/berita/d-7853708/detik-detik-kaki-korban-ditemukan-tertimbun-longsor-jalur-pacet-cangar

[5] gridoto.com, "Hampir Rampung, Pengerjaan Tol Cisumdawu Seksi 2 Terkendala Masalah Ini," 2022. https://otomotifnet.gridoto.com/read/233154679/hampir-rampung-pengerjaan-tol-cisumdawu-seksi-2-terkendala-masalah-ini

[6] A. Ajraoui *et al.*, "Geotechnical Analysis and Stabilization of the Jebha Landslide: A Case Study from Morocco's Mediterranean Ring Road," *Civ. Eng. Archit.*, vol. 13, no. 2, pp. 949–964, 2025, doi: 10.13189/cea.2025.130214.

[7] S. Das, S. Saraswat, B. K. Maheshwari, and R. S. Jakka, "Geotechnical Investigations

ISSN (*Online*) 2581-0855
ISSN (*Print*) 2579-4620

for Land Subsidence in Joshimath, Uttarakhand," *Indian Geotech. J.*, no. 0123456789, 2025, doi: 10.1007/s40098-024-01153-8.

[8] D. Khadka, J. Zhang, and A. Sharma, "Geographic object-based image analysis for landslide identification using machine learning on google earth engine," *Environ. Earth Sci.*, vol. 84, no. 3, pp. 1–27, 2025, doi: 10.1007/s12665-024-12045-8.

[9] N. Badavath and S. Sahoo, "Geospatial assessment and integrated multi-model approach for landslide susceptibility mapping in Meghalaya, India," *Adv. Sp. Res.*, vol. 75, no. 3, pp. 2764–2791, 2024, doi: 10.1016/j.asr.2024.11.052.

[10] B. Demirel, E. Yildirim, and E. Can, "GIS-based landslide susceptibility mapping using AHP, FMEA, and Pareto systematic analysis in central Yalova, Türkiye," *Eng. Sci. Technol. an Int. J.*, vol. 64, no. November 2024, p. 102013, 2025, doi: 10.1016/j.jestch.2025.102013.

[11] C. Xiaoting, D. Xingchen, L. Jianwei, L. Guowei, and L. Shuqiang, "Mechanics and Dynamics of the Xintan Landslide: Insights from Geological Factors and Simulations," *Geotech. Geol. Eng.*, vol. 43, no. 2, pp. 1–16, 2025, doi: 10.1007/s10706-024-02998-9.

[12] Y. Cao, H. Li, C. Long, G. Yang, C. Zhang, and D. Peng, "Stability Analysis and Reinforcement Management of Slope," in *E3S Web of Conferences*, 2023. doi: 10.1051/e3sconf/202340604031.

[13] R. Genevois, P. R. Tecca, and C. Genevois, "Mitigation measures of debris flow and landslide risk carried out in two mountain areas of North-Eastern Italy," *J. Mt. Sci.*, vol. 19, no. 6, pp. 1808–1822, 2022, doi: 10.1007/s11629-021-7212-6.

[14] U. Prasad, P. N. Alarcon, and J. Franquet, "New method of XRF/XRD based mineralogy for estimating matrix-modulus, Biot's-coefficient and effective-stress using VRH and HS bounds of rock physics principles," in *58th US Rock Mechanics / Geomechanics Symposium 2024, ARMA 2024*, 2024. doi: 10.56952/ARMA-2024-0804.

[15] Z. Ouyang, P. W. Mayne, and S. Agaiby, "In situ test-based evaluation of soil effective stress strength properties and stress history," in *Databases for Data-Centric Geotechnics: Site Characterization*, 2024, pp. 344–368. doi: 10.1201/9781003441946-12.

[16] W. Powrie, "Groundwater profiles and effective stresses," in *ICE Manual of Geotechnical Engineering: Second Edition*, 2023, pp. 183–186. doi: 10.1680/icemge.66816.0183.

[17] S. Yasar, "Long term wetting characteristics and saturation induced strength reduction of some igneous rocks," *Environ. Earth Sci.*, vol. 79, no. 14, 2020, doi: 10.1007/s12665-

https://dx.doi.org/10.30737/ukarst.v9i1.6587

U Karst
Volume 09 Number 01 Year 2025
ISSN (*Online*) 2581-0855
ISSN (*Print*) 2579-4620

020-09105-0.

[18] M. J. Heap *et al.*, "The influence of water-saturation on the strength of volcanic rocks and the stability of lava domes," *J. Volcanol. Geotherm. Res.*, vol. 444, 2023, doi: 10.1016/j.jvolgeores.2023.107962.

[19] R. Baltodano-Goulding and L. Brenes-Garcia, "Influence of Degree of Saturation on the Dynamic Soil Properties of a Fine-Grained Soil," in *Geotechnical Special Publication*, 2022, pp. 541–548. doi: 10.1061/9780784484043.052.

[20] O. Hernandez, M. P. Cordão Neto, and B. Caicedo, "Structural features and hydro-mechanical behaviour of a compacted andesitic volcanic soil," *Geotech. Lett.*, vol. 8, no. 3, pp. 195–200, 2018, doi: 10.1680/jgele.18.00056.

[21] B. Jatmika, A. Darmawan, D. Hikmah, D. Husen, and S. S. Suri, "Soil Endurance Analysis Using Soil Nailing Method to Strengten Slope Landscape," in *6th International Conference on Computing, Engineering, and Design, ICCED 2020*, 2020. doi: 10.1109/ICCED51276.2020.9415758.

[22] A. R. Kalantari, A. Johari, M. Zandpour, and M. Kalantari, "Effect of spatial variability of soil properties and geostatistical conditional simulation on reliability characteristics and critical slip surfaces of soil slopes," *Transp. Geotech.*, vol. 39, 2023, doi: 10.1016/j.trgeo.2023.100933.

[23] A. Troncone, L. Pugliese, A. Parise, and E. Conte, "A simple method to reduce mesh dependency in modelling landslides involving brittle soils," *Geotech. Lett.*, vol. 12, no. 3, 2022, doi: 10.1680/jgele.22.00023.

[24] J. Fei, D. Peng, Y. Jie, Z. Guo, and X. Chen, "Hybrid Finite-Element Material-Point Method for Reinforced Slopes," *Comput. Geotech.*, vol. 172, 2024, doi: 10.1016/j.compgeo.2024.106428.

[25] W. Lyu, S. Yang, W. Xin, X. Sun, J. Zhang, and G. Bo, "Study on linear prediction method of pumped aquifer compression based on coupling process," *J. For. Eng.*, vol. 6, no. 3, pp. 154–160, 2021, doi: 10.13360/j.issn.2096-l359.202007013.

[26] O. T. Faloye, A. E. Ajayi, A. Zink, H. Fleige, J. Dörner, and R. Horn, "Effective stress and pore water dynamics in unsaturated soils: Influence of soil compaction history and soil properties," *Soil Tillage Res.*, vol. 211, 2021, doi: 10.1016/j.still.2021.104997.

[27] L. Shao, X. Guo, T. Wen, and B. Zhao, "Effective Stress and Effective Stress Equation," in *Springer Series in Geomechanics and Geoengineering*, 2019, pp. 175–192. doi: 10.1007/978-3-030-14987-1_22.